SLAC-PUB-12009
BABAR-CONF-06/041

arXiv:hep-ex/0607100v1 29 Jul 2006

Time-dependent CP-violation parameters in $B^0 \to \eta' K^0$ decay

The *BABAR* Collaboration

February 7, 2008

Abstract

We present measurements of time-dependent CP-violation asymmetries for the decays $B^0 \to \eta' K^0$. The data sample corresponds to 347 million $B\overline{B}$ pairs produced by e^+e^- annihilation at the $\Upsilon(4S)$ resonance in the PEP-II collider, and collected with the *BABAR* detector. The preliminary results are $S = 0.55 \pm 0.11 \pm 0.02$, and $C = -0.15 \pm 0.07 \pm 0.03$, where the first error quoted is statistical, the second systematic.

Submitted to the 33rd International Conference on High-Energy Physics, ICHEP 06, 26 July—2 August 2006, Moscow, Russia.

Stanford Linear Accelerator Center, Stanford University, Stanford, CA 94309

Work supported in part by Department of Energy contract DE-AC03-76SF00515.

The *BABAR* Collaboration,

B. Aubert, R. Barate, M. Bona, D. Boutigny, F. Couderc, Y. Karyotakis, J. P. Lees, V. Poireau, V. Tisserand, A. Zghiche

Laboratoire de Physique des Particules, IN2P3/CNRS et Université de Savoie, F-74941 Annecy-Le-Vieux, France

E. Grauges

Universitat de Barcelona, Facultat de Fisica, Departament ECM, E-08028 Barcelona, Spain

A. Palano

Università di Bari, Dipartimento di Fisica and INFN, I-70126 Bari, Italy

J. C. Chen, N. D. Qi, G. Rong, P. Wang, Y. S. Zhu

Institute of High Energy Physics, Beijing 100039, China

G. Eigen, I. Ofte, B. Stugu

University of Bergen, Institute of Physics, N-5007 Bergen, Norway

G. S. Abrams, M. Battaglia, D. N. Brown, J. Button-Shafer, R. N. Cahn, E. Charles, M. S. Gill, Y. Groysman, R. G. Jacobsen, J. A. Kadyk, L. T. Kerth, Yu. G. Kolomensky, G. Kukartsev, G. Lynch, L. M. Mir, T. J. Orimoto, M. Pripstein, N. A. Roe, M. T. Ronan, W. A. Wenzel

Lawrence Berkeley National Laboratory and University of California, Berkeley, California 94720, USA

P. del Amo Sanchez, M. Barrett, K. E. Ford, A. J. Hart, T. J. Harrison, C. M. Hawkes, S. E. Morgan, A. T. Watson

University of Birmingham, Birmingham, B15 2TT, United Kingdom

T. Held, H. Koch, B. Lewandowski, M. Pelizaeus, K. Peters, T. Schroeder, M. Steinke

Ruhr Universität Bochum, Institut für Experimentalphysik 1, D-44780 Bochum, Germany

J. T. Boyd, J. P. Burke, W. N. Cottingham, D. Walker

University of Bristol, Bristol BS8 1TL, United Kingdom

D. J. Asgeirsson, T. Cuhadar-Donszelmann, B. G. Fulsom, C. Hearty, N. S. Knecht, T. S. Mattison, J. A. McKenna

University of British Columbia, Vancouver, British Columbia, Canada V6T 1Z1

A. Khan, P. Kyberd, M. Saleem, D. J. Sherwood, L. Teodorescu

Brunel University, Uxbridge, Middlesex UB8 3PH, United Kingdom

V. E. Blinov, A. D. Bukin, V. P. Druzhinin, V. B. Golubev, A. P. Onuchin, S. I. Serednyakov, Yu. I. Skovpen, E. P. Solodov, K. Yu Todyshev

Budker Institute of Nuclear Physics, Novosibirsk 630090, Russia

D. S. Best, M. Bondioli, M. Bruinsma, M. Chao, S. Curry, I. Eschrich, D. Kirkby, A. J. Lankford, P. Lund, M. Mandelkern, R. K. Mommsen, W. Roethel, D. P. Stoker

University of California at Irvine, Irvine, California 92697, USA

S. Abachi, C. Buchanan

University of California at Los Angeles, Los Angeles, California 90024, USA

S. D. Foulkes, J. W. Gary, O. Long, B. C. Shen, K. Wang, L. Zhang
University of California at Riverside, Riverside, California 92521, USA

H. K. Hadavand, E. J. Hill, H. P. Paar, S. Rahatlou, V. Sharma
University of California at San Diego, La Jolla, California 92093, USA

J. W. Berryhill, C. Campagnari, A. Cunha, B. Dahmes, T. M. Hong, D. Kovalskyi, J. D. Richman
University of California at Santa Barbara, Santa Barbara, California 93106, USA

T. W. Beck, A. M. Eisner, C. J. Flacco, C. A. Heusch, J. Kroseberg, W. S. Lockman, G. Nesom, T. Schalk, B. A. Schumm, A. Seiden, P. Spradlin, D. C. Williams, M. G. Wilson
University of California at Santa Cruz, Institute for Particle Physics, Santa Cruz, California 95064, USA

J. Albert, E. Chen, A. Dvoretskii, F. Fang, D. G. Hitlin, I. Narsky, T. Piatenko, F. C. Porter, A. Ryd, A. Samuel
California Institute of Technology, Pasadena, California 91125, USA

G. Mancinelli, B. T. Meadows, K. Mishra, M. D. Sokoloff
University of Cincinnati, Cincinnati, Ohio 45221, USA

F. Blanc, P. C. Bloom, S. Chen, W. T. Ford, J. F. Hirschauer, A. Kreisel, M. Nagel, U. Nauenberg, A. Olivas, W. O. Ruddick, J. G. Smith, K. A. Ulmer, S. R. Wagner, J. Zhang
University of Colorado, Boulder, Colorado 80309, USA

A. Chen, E. A. Eckhart, A. Soffer, W. H. Toki, R. J. Wilson, F. Winklmeier, Q. Zeng
Colorado State University, Fort Collins, Colorado 80523, USA

D. D. Altenburg, E. Feltresi, A. Hauke, H. Jasper, J. Merkel, A. Petzold, B. Spaan
Universität Dortmund, Institut für Physik, D-44221 Dortmund, Germany

T. Brandt, V. Klose, H. M. Lacker, W. F. Mader, R. Nogowski, J. Schubert, K. R. Schubert, R. Schwierz, J. E. Sundermann, A. Volk
Technische Universität Dresden, Institut für Kern- und Teilchenphysik, D-01062 Dresden, Germany

D. Bernard, G. R. Bonneaud, E. Latour, Ch. Thiebaux, M. Verderi
Laboratoire Leprince-Ringuet, CNRS/IN2P3, Ecole Polytechnique, F-91128 Palaiseau, France

P. J. Clark, W. Gradl, F. Muheim, S. Playfer, A. I. Robertson, Y. Xie
University of Edinburgh, Edinburgh EH9 3JZ, United Kingdom

M. Andreotti, D. Bettoni, C. Bozzi, R. Calabrese, G. Cibinetto, E. Luppi, M. Negrini, A. Petrella, L. Piemontese, E. Prencipe
Università di Ferrara, Dipartimento di Fisica and INFN, I-44100 Ferrara, Italy

F. Anulli, R. Baldini-Ferroli, A. Calcaterra, R. de Sangro, G. Finocchiaro, S. Pacetti, P. Patteri, I. M. Peruzzi,[1] M. Piccolo, M. Rama, A. Zallo
Laboratori Nazionali di Frascati dell'INFN, I-00044 Frascati, Italy

[1]Also with Università di Perugia, Dipartimento di Fisica, Perugia, Italy

A. Buzzo, R. Capra, R. Contri, M. Lo Vetere, M. M. Macri, M. R. Monge, S. Passaggio, C. Patrignani, E. Robutti, A. Santroni, S. Tosi

Università di Genova, Dipartimento di Fisica and INFN, I-16146 Genova, Italy

G. Brandenburg, K. S. Chaisanguanthum, M. Morii, J. Wu

Harvard University, Cambridge, Massachusetts 02138, USA

R. S. Dubitzky, J. Marks, S. Schenk, U. Uwer

Universität Heidelberg, Physikalisches Institut, Philosophenweg 12, D-69120 Heidelberg, Germany

D. J. Bard, W. Bhimji, D. A. Bowerman, P. D. Dauncey, U. Egede, R. L. Flack, J. A. Nash, M. B. Nikolich, W. Panduro Vazquez

Imperial College London, London, SW7 2AZ, United Kingdom

P. K. Behera, X. Chai, M. J. Charles, U. Mallik, N. T. Meyer, V. Ziegler

University of Iowa, Iowa City, Iowa 52242, USA

J. Cochran, H. B. Crawley, L. Dong, V. Eyges, W. T. Meyer, S. Prell, E. I. Rosenberg, A. E. Rubin

Iowa State University, Ames, Iowa 50011-3160, USA

A. V. Gritsan

Johns Hopkins University, Baltimore, Maryland 21218, USA

A. G. Denig, M. Fritsch, G. Schott

Universität Karlsruhe, Institut für Experimentelle Kernphysik, D-76021 Karlsruhe, Germany

N. Arnaud, M. Davier, G. Grosdidier, A. Höcker, F. Le Diberder, V. Lepeltier, A. M. Lutz, A. Oyanguren, S. Pruvot, S. Rodier, P. Roudeau, M. H. Schune, A. Stocchi, W. F. Wang, G. Wormser

Laboratoire de l'Accélérateur Linéaire, IN2P3/CNRS et Université Paris-Sud 11, Centre Scientifique d'Orsay, B.P. 34, F-91898 ORSAY Cedex, France

C. H. Cheng, D. J. Lange, D. M. Wright

Lawrence Livermore National Laboratory, Livermore, California 94550, USA

C. A. Chavez, I. J. Forster, J. R. Fry, E. Gabathuler, R. Gamet, K. A. George, D. E. Hutchcroft, D. J. Payne, K. C. Schofield, C. Touramanis

University of Liverpool, Liverpool L69 7ZE, United Kingdom

A. J. Bevan, F. Di Lodovico, W. Menges, R. Sacco

Queen Mary, University of London, E1 4NS, United Kingdom

G. Cowan, H. U. Flaecher, D. A. Hopkins, P. S. Jackson, T. R. McMahon, S. Ricciardi, F. Salvatore, A. C. Wren

University of London, Royal Holloway and Bedford New College, Egham, Surrey TW20 0EX, United Kingdom

D. N. Brown, C. L. Davis

University of Louisville, Louisville, Kentucky 40292, USA

J. Allison, N. R. Barlow, R. J. Barlow, Y. M. Chia, C. L. Edgar, G. D. Lafferty, M. T. Naisbit, J. C. Williams, J. I. Yi

University of Manchester, Manchester M13 9PL, United Kingdom

C. Chen, W. D. Hulsbergen, A. Jawahery, C. K. Lae, D. A. Roberts, G. Simi

University of Maryland, College Park, Maryland 20742, USA

G. Blaylock, C. Dallapiccola, S. S. Hertzbach, X. Li, T. B. Moore, S. Saremi, H. Staengle

University of Massachusetts, Amherst, Massachusetts 01003, USA

R. Cowan, G. Sciolla, S. J. Sekula, M. Spitznagel, F. Taylor, R. K. Yamamoto

Massachusetts Institute of Technology, Laboratory for Nuclear Science, Cambridge, Massachusetts 02139, USA

H. Kim, S. E. Mclachlin, P. M. Patel, S. H. Robertson

McGill University, Montréal, Québec, Canada H3A 2T8

A. Lazzaro, V. Lombardo, F. Palombo

Università di Milano, Dipartimento di Fisica and INFN, I-20133 Milano, Italy

J. M. Bauer, L. Cremaldi, V. Eschenburg, R. Godang, R. Kroeger, D. A. Sanders, D. J. Summers, H. W. Zhao

University of Mississippi, University, Mississippi 38677, USA

S. Brunet, D. Côté, M. Simard, P. Taras, F. B. Viaud

Université de Montréal, Physique des Particules, Montréal, Québec, Canada H3C 3J7

H. Nicholson

Mount Holyoke College, South Hadley, Massachusetts 01075, USA

N. Cavallo,[2] G. De Nardo, F. Fabozzi,[3] C. Gatto, L. Lista, D. Monorchio, P. Paolucci, D. Piccolo, C. Sciacca

Università di Napoli Federico II, Dipartimento di Scienze Fisiche and INFN, I-80126, Napoli, Italy

M. A. Baak, G. Raven, H. L. Snoek

NIKHEF, National Institute for Nuclear Physics and High Energy Physics, NL-1009 DB Amsterdam, The Netherlands

C. P. Jessop, J. M. LoSecco

University of Notre Dame, Notre Dame, Indiana 46556, USA

T. Allmendinger, G. Benelli, L. A. Corwin, K. K. Gan, K. Honscheid, D. Hufnagel, P. D. Jackson, H. Kagan, R. Kass, A. M. Rahimi, J. J. Regensburger, R. Ter-Antonyan, Q. K. Wong

Ohio State University, Columbus, Ohio 43210, USA

N. L. Blount, J. Brau, R. Frey, O. Igonkina, J. A. Kolb, M. Lu, R. Rahmat, N. B. Sinev, D. Strom, J. Strube, E. Torrence

University of Oregon, Eugene, Oregon 97403, USA

[2]Also with Università della Basilicata, Potenza, Italy
[3]Also with Università della Basilicata, Potenza, Italy

A. Gaz, M. Margoni, M. Morandin, A. Pompili, M. Posocco, M. Rotondo, F. Simonetto, R. Stroili, C. Voci

Università di Padova, Dipartimento di Fisica and INFN, I-35131 Padova, Italy

M. Benayoun, H. Briand, J. Chauveau, P. David, L. Del Buono, Ch. de la Vaissière, O. Hamon, B. L. Hartfiel, M. J. J. John, Ph. Leruste, J. Malclès, J. Ocariz, L. Roos, G. Therin

Laboratoire de Physique Nucléaire et de Hautes Energies, IN2P3/CNRS, Université Pierre et Marie Curie-Paris6, Université Denis Diderot-Paris7, F-75252 Paris, France

L. Gladney, J. Panetta

University of Pennsylvania, Philadelphia, Pennsylvania 19104, USA

M. Biasini, R. Covarelli

Università di Perugia, Dipartimento di Fisica and INFN, I-06100 Perugia, Italy

C. Angelini, G. Batignani, S. Bettarini, F. Bucci, G. Calderini, M. Carpinelli, R. Cenci, F. Forti, M. A. Giorgi, A. Lusiani, G. Marchiori, M. A. Mazur, M. Morganti, N. Neri, E. Paoloni, G. Rizzo, J. J. Walsh

Università di Pisa, Dipartimento di Fisica, Scuola Normale Superiore and INFN, I-56127 Pisa, Italy

M. Haire, D. Judd, D. E. Wagoner

Prairie View A&M University, Prairie View, Texas 77446, USA

J. Biesiada, N. Danielson, P. Elmer, Y. P. Lau, C. Lu, J. Olsen, A. J. S. Smith, A. V. Telnov

Princeton University, Princeton, New Jersey 08544, USA

F. Bellini, G. Cavoto, A. D'Orazio, D. del Re, E. Di Marco, R. Faccini, F. Ferrarotto, F. Ferroni, M. Gaspero, L. Li Gioi, M. A. Mazzoni, S. Morganti, G. Piredda, F. Polci, F. Safai Tehrani, C. Voena

Università di Roma La Sapienza, Dipartimento di Fisica and INFN, I-00185 Roma, Italy

M. Ebert, H. Schröder, R. Waldi

Universität Rostock, D-18051 Rostock, Germany

T. Adye, N. De Groot, B. Franek, E. O. Olaiya, F. F. Wilson

Rutherford Appleton Laboratory, Chilton, Didcot, Oxon, OX11 0QX, United Kingdom

R. Aleksan, S. Emery, A. Gaidot, S. F. Ganzhur, G. Hamel de Monchenault, W. Kozanecki, M. Legendre, G. Vasseur, Ch. Yèche, M. Zito

DSM/Dapnia, CEA/Saclay, F-91191 Gif-sur-Yvette, France

X. R. Chen, H. Liu, W. Park, M. V. Purohit, J. R. Wilson

University of South Carolina, Columbia, South Carolina 29208, USA

M. T. Allen, D. Aston, R. Bartoldus, P. Bechtle, N. Berger, R. Claus, J. P. Coleman, M. R. Convery, M. Cristinziani, J. C. Dingfelder, J. Dorfan, G. P. Dubois-Felsmann, D. Dujmic, W. Dunwoodie, R. C. Field, T. Glanzman, S. J. Gowdy, M. T. Graham, P. Grenier,[4] V. Halyo, C. Hast, T. Hryn'ova, W. R. Innes, M. H. Kelsey, P. Kim, D. W. G. S. Leith, S. Li, S. Luitz, V. Luth, H. L. Lynch, D. B. MacFarlane, H. Marsiske, R. Messner, D. R. Muller, C. P. O'Grady, V. E. Ozcan, A. Perazzo, M. Perl, T. Pulliam, B. N. Ratcliff, A. Roodman, A. A. Salnikov, R. H. Schindler, J. Schwiening, A. Snyder, J. Stelzer, D. Su, M. K. Sullivan, K. Suzuki, S. K. Swain, J. M. Thompson, J. Va'vra, N. van

[4]Also at Laboratoire de Physique Corpusculaire, Clermont-Ferrand, France

Bakel, M. Weaver, A. J. R. Weinstein, W. J. Wisniewski, M. Wittgen, D. H. Wright, A. K. Yarritu, K. Yi, C. C. Young

Stanford Linear Accelerator Center, Stanford, California 94309, USA

P. R. Burchat, A. J. Edwards, S. A. Majewski, B. A. Petersen, C. Roat, L. Wilden

Stanford University, Stanford, California 94305-4060, USA

S. Ahmed, M. S. Alam, R. Bula, J. A. Ernst, V. Jain, B. Pan, M. A. Saeed, F. R. Wappler, S. B. Zain

State University of New York, Albany, New York 12222, USA

W. Bugg, M. Krishnamurthy, S. M. Spanier

University of Tennessee, Knoxville, Tennessee 37996, USA

R. Eckmann, J. L. Ritchie, A. Satpathy, C. J. Schilling, R. F. Schwitters

University of Texas at Austin, Austin, Texas 78712, USA

J. M. Izen, X. C. Lou, S. Ye

University of Texas at Dallas, Richardson, Texas 75083, USA

F. Bianchi, F. Gallo, D. Gamba

Università di Torino, Dipartimento di Fisica Sperimentale and INFN, I-10125 Torino, Italy

M. Bomben, L. Bosisio, C. Cartaro, F. Cossutti, G. Della Ricca, S. Dittongo, L. Lanceri, L. Vitale

Università di Trieste, Dipartimento di Fisica and INFN, I-34127 Trieste, Italy

V. Azzolini, N. Lopez-March, F. Martinez-Vidal

IFIC, Universitat de Valencia-CSIC, E-46071 Valencia, Spain

Sw. Banerjee, B. Bhuyan, C. M. Brown, D. Fortin, K. Hamano, R. Kowalewski, I. M. Nugent, J. M. Roney, R. J. Sobie

University of Victoria, Victoria, British Columbia, Canada V8W 3P6

J. J. Back, P. F. Harrison, T. E. Latham, G. B. Mohanty, M. Pappagallo

Department of Physics, University of Warwick, Coventry CV4 7AL, United Kingdom

H. R. Band, X. Chen, B. Cheng, S. Dasu, M. Datta, K. T. Flood, J. J. Hollar, P. E. Kutter, B. Mellado, A. Mihalyi, Y. Pan, M. Pierini, R. Prepost, S. L. Wu, Z. Yu

University of Wisconsin, Madison, Wisconsin 53706, USA

H. Neal

Yale University, New Haven, Connecticut 06511, USA

1 INTRODUCTION

Measurements of time-dependent *CP* asymmetries in B^0 meson decays through a dominant Cabibbo-Kobayashi-Maskawa (CKM) favored $b \to c\bar{c}s$ amplitude [1] have provided a crucial test of the mechanism of *CP* violation in the Standard Model (SM) [2]. For such decays the interference between this amplitude and $B^0\overline{B}^0$ mixing is dominated by the single phase $\beta = \arg\left(-V_{cd}V_{cb}^*/V_{td}V_{tb}^*\right)$ of the CKM mixing matrix. Decays of B^0 mesons to charmless hadronic final states such as $\eta' K^0$ proceed mostly via a single loop (penguin) amplitude with the same weak phase as the $b \to c\bar{c}s$ transition [3], but CKM-suppressed amplitudes and multiple particles in the loop introduce additional weak phases whose contribution may not be negligible [4, 5, 6, 7, 8].

For the decay $B^0 \to \eta' K^0$, these additional contributions are expected to be small within the SM, so the time-dependent asymmetry measurement for this decay provides an approximate measurement of $\sin 2\beta$. Theoretical bounds for the small deviation ΔS between the time-dependent *CP*-violation parameter S measured in this decay and in the charmonium-K^0 decays have been calculated with an SU(3) analysis [4, 5] from measurements of B^0 decays to pairs of neutral light pseudoscalar mesons [9, 10]. The most stringent of these is given by Eq. 19 in [5], which assumes negligible contributions from exchange and penguin annihilation, and has a theoretical uncertainty less than $\sim$0.03. With newer measurements [11] we obtain an improved bound $\Delta S < 0.08$ [12]. QCD factorization calculations conclude that ΔS is even smaller [7]. A significantly larger ΔS could arise from non-SM amplitudes [8].

The time-dependent *CP*-violation asymmetry in the decay $B^0 \to \eta' K^0$ has been measured previously by the *BABAR* [13] and Belle [14, 15] experiments. In this paper we update our previous measurements with an improved analysis and a data sample 1.5 times larger.

2 THE *BABAR* DETECTOR AND DATASET

The data were collected with the *BABAR* detector [16] at the PEP-II asymmetric-energy e^+e^- collider [17]. An integrated luminosity of 316 fb^{-1}, corresponding to 347 million $B\overline{B}$ pairs, was recorded at the $\Upsilon(4S)$ resonance (center-of-mass energy $\sqrt{s} = 10.58$ GeV).

Charged particles from e^+e^- interactions are detected, and their momenta measured, by a combination of five layers of double-sided silicon microstrip detectors and a 40-layer drift chamber, both operating in the 1.5 T magnetic field of a superconducting solenoid. Photons and electrons are identified with a CsI(Tl) electromagnetic calorimeter (EMC). Further charged particle identification (PID) is provided by the average energy loss (dE/dx) in the tracking devices and by an internally reflecting ring imaging Cherenkov detector (DIRC) covering the central region. The instrumented flux return (IFR) of the magnet allows discrimination of muons from pions.

3 ANALYSIS METHOD

3.1 Time evolution of a $B^0\overline{B}^0$ pair

From a candidate $B\overline{B}$ pair we reconstruct a B^0 decaying into the *CP* eigenstate $f = \eta' K_S^0$ or $f = \eta' K_L^0$ (B_{CP}). From the remaining particles in the event we also reconstruct the vertex of the other B meson ($B_{\rm tag}$) and identify its flavor. The difference $\Delta t \equiv t_{CP} - t_{\rm tag}$ of the proper decay times t_{CP} and $t_{\rm tag}$ of the signal and tag B mesons, respectively, is obtained from the measured distance between the B_{CP} and $B_{\rm tag}$ decay vertices and from the boost ($\beta\gamma = 0.56$) of the e^+e^-

Table 1: Selection requirements on the invariant masses of resonances and the laboratory energies of photons from their decay.

State	Invariant mass (MeV)	$E(\gamma)$ (MeV)
π^0 (from $\eta_{3\pi}$)	$120 < m(\gamma\gamma) < 150$	> 30
π^0 (from K^0_{S00})	$120 < m(\gamma\gamma) < 155$	> 30
$\eta_{\gamma\gamma}$	$490 < m(\gamma\gamma) < 600$	> 50
$\eta_{3\pi}$	$520 < m(\pi^+\pi^-\pi^0) < 570$	—
$\eta'_{\eta\pi\pi}$	$945 < m(\pi^+\pi^-\eta) < 970$	—
$\eta'_{\rho\gamma}$	$930 < m(\pi^+\pi^-\gamma) < 980$	> 100
ρ^0	$470 < m(\pi^+\pi^-) < 980$	—
K^0_{S+-}	$486 < m(\pi^+\pi^-) < 510$	—
K^0_{S00}	$468 < m(\pi^0\pi^0) < 528$	—

system. The Δt distribution is given by:

$$F(\Delta t) = \frac{e^{-|\Delta t|/\tau}}{4\tau}[1 \mp \Delta w \pm (1-2w)\,(S\sin(\Delta m_d \Delta t) - C\cos(\Delta m_d \Delta t))]. \quad (1)$$

The upper (lower) sign denotes a decay accompanied by a B^0 ($\overline{B}^0$) tag, τ is the mean B^0 lifetime, Δm_d is the mixing frequency, and the mistag parameters w and Δw are the average and difference, respectively, of the probabilities that a true B^0 is incorrectly tagged as a $\overline{B}^0$ or vice versa. The tagging algorithm [18] has six mutually exclusive tagging categories based on quantities such as the sign of charge of a lepton, kaon, or soft pion from D^*, grouped according to their response purities. The measured analyzing power, defined as efficiency times $(1-2w)^2$ summed over all categories, is (30.4±0.3)%, as determined from a large sample of B-decays to fully reconstructed flavor eigenstates ($B_{\rm flav}$). The parameter C measures direct CP violation. If $C = 0$, then $S = -\eta \sin 2\beta + \Delta S$, where η is the CP eigenvalue of the final state (-1 for $\eta' K^0_S$, $+1$ for $\eta' K^0_L$).

3.2 Event selection

We establish the event selection criteria with the aid of a detailed Monte Carlo (MC) simulation of the B production and decay sequences, and of the detector response [19]. These criteria are designed to retain signal events with high efficiency. Applied to the data, they result in a sample much larger than the expected signal, but with well characterized backgrounds. We extract the signal yields from this sample with a maximum likelihood (ML) fit.

The B-daughter candidates are reconstructed through their decays $\pi^0 \to \gamma\gamma$, $\eta \to \gamma\gamma$ ($\eta_{\gamma\gamma}$), $\eta \to \pi^+\pi^-\pi^0$ ($\eta_{3\pi}$), $\eta' \to \eta_{\gamma\gamma}\pi^+\pi^-$ ($\eta'_{\eta(\gamma\gamma)\pi\pi}$), $\eta' \to \eta_{3\pi}\pi^+\pi^-$ ($\eta'_{\eta(3\pi)\pi\pi}$), $\eta' \to \rho^0\gamma$ ($\eta'_{\rho\gamma}$), where $\rho^0 \to \pi^+\pi^-$, $K^0_S \to \pi^+\pi^-$ (K^0_{S+-}) or $\pi^0\pi^0$ (K^0_{S00}). Table 1 lists the requirements on the invariant mass of these particles' final states. Secondary charged pions in η' and η candidates are rejected if classified as protons, kaons, or electrons by their DIRC, dE/dx, and EMC PID signatures. We require K^0_S candidates to have a flight length with significance $>3\sigma$. Signal K^0_L candidates are reconstructed from clusters of energy deposited in the EMC or from hits in the IFR not associated with any charged track in the event. From the cluster centroid and the B^0 decay vertex we determine the direction (but not the magnitude) of the K^0_L momentum $\mathbf{p}_{K^0_L}$.

For decays with a K^0_S we reconstruct the B-meson candidate by combining the four-momenta of the K^0_S and η' and imposing a vertex constraint. Since the natural widths of the η, η', and π^0 are much smaller than the resolution, we also constrain their masses to world-average values [20] in the fit of the B candidate. From the kinematics of $\Upsilon(4S)$ decay we determine the energy-substituted mass $m_{\rm ES} \equiv \sqrt{(\frac{1}{2}s + \mathbf{p}_0 \cdot \mathbf{p}_B)^2/E_0^2 - \mathbf{p}_B^2}$ and the energy difference $\Delta E \equiv E_B^* - \frac{1}{2}\sqrt{s}$, where $(E_0, \mathbf{p}_0)$ and $(E_B, \mathbf{p}_B)$ are four-momenta of the $\Upsilon(4S)$ and the B candidate, respectively, and the asterisk denotes the $\Upsilon(4S)$ rest frame. The resolution in $m_{\rm ES}$ is 3.0 MeV and in ΔE is $20 - 50$ MeV, depending on the decay mode. We require $5.25 < m_{\rm ES} < 5.29$ GeV and $|\Delta E| < 0.2$ GeV ($-0.01 < \Delta E < 0.08$ GeV for $B^0 \to \eta' K^0_L$).

For a $B^0 \to \eta' K^0_L$ candidate we obtain ΔE and $p_{K^0_L}$ from a fit with B^0 and K^0_L masses constrained to their accepted values [20]. To make a match with the measured K^0_L direction we construct the missing momentum $\mathbf{p}_{\rm miss}$ from $\mathbf{p}_0$ and all charged tracks and neutral clusters other than the K^0_L. We then project $\mathbf{p}_{\rm miss}$ onto $\mathbf{p}_{K^0_L}$, and require the component perpendicular to the beam line, $\mathbf{p}^{\rm proj}_{{\rm miss}\perp}$, to satisfy $p^{\rm proj}_{{\rm miss}\perp} - p_{K^0_L\perp} > -0.5$ GeV/c. This value reflects the resolution, and was chosen to minimize the yield uncertainty in the presence of continuum background.

For all $B^0 \to \eta' K^0$ candidates we require for Δt and its error $\sigma_{\Delta t}$, $|\Delta t| < 20$ ps and $\sigma_{\Delta t} < 2.5$ ps.

3.3 Background rejection

Backgrounds arise primarily from random combinations of particles in continuum $e^+e^- \to q\overline{q}$ events ($q = u, d, s, c$). We reduce these with requirements on the angle $\theta_{\rm T}$ between the thrust axis of the B candidate in the $\Upsilon(4S)$ frame and that of the rest of the charged tracks and neutral calorimeter clusters in the event. The distribution is sharply peaked near $|\cos\theta_{\rm T}| = 1$ for $q\overline{q}$ jet pairs, and nearly uniform for B-meson decays. The requirement, which optimizes the expected signal yield relative to its background-dominated statistical error, is $|\cos\theta_{\rm T}| < 0.9$ ($|\cos\theta_{\rm T}| < 0.8$ for $B^0 \to \eta' K^0_L$).

In the ML fit we discriminate further against $q\overline{q}$ background with a Fisher discriminant $\mathcal{F}$ that combines several variables which characterize the production dynamics and energy flow in the event [10]. It provides about one standard deviation of separation between B decay events and combinatorial background.

For the $\eta'_{\rho\gamma}$ decays we require $|\cos\theta^\rho_{\rm dec}| < 0.9$ to exclude the most asymmetric decays where soft-particle backgrounds concentrate and the acceptance changes rapidly. Here $\theta^\rho_{\rm dec}$ is the angle between the momenta of the ρ^0 daughter π^- and the η', measured in the ρ^0 rest frame.

For $B^0 \to \eta' K^0_L$ candidates we require that the cosine of the polar angle of the total missing momentum in the laboratory system be less than 0.95, to reject very forward $q\overline{q}$ jets. The purity of the K^0_L candidates reconstructed in the EMC is further improved by a requirement on the output of a neural network (NN) that takes cluster-shape variables as its inputs. The NN was trained on MC signal events and data events in the sideband $0.04 < \Delta E < 0.08$ GeV. We checked the performance of the NN with K^0_L candidates in the larger $B^0 \to J/\psi K^0_L$ sample.

The average number of candidates found per selected event is in the range 1.08 to 1.32, depending on the final state. We choose the candidate with the smallest value of a χ^2 constructed from the deviations from expected values of one or more of the daughter resonance masses, or with the best vertex probability for the B, depending on the decay channel. In $B^0 \to \eta' K^0_L$ if several B candidates have the same vertex probability, we chose the candidate with the K^0_L reconstructed from, in order, EMC and IFR, EMC only, or IFR only. From the simulation we find that this algorithm selects the correct-combination candidate in about two thirds of the events containing

multiple candidates, and that it induces negligible bias.

3.4 Maximum likelihood fit

We obtain the common *CP*-violation parameters and yields for each channel from a maximum likelihood fit with the input observables ΔE, $m_{\rm ES}$, $\mathcal{F}$, and Δt. The selected sample sizes are given in the first column of Table 2. Besides the signal events they contain $q\overline{q}$ (dominant) and $b\overline{b}$ with $b \to c$ combinatorial background, and a fraction that we estimate from the simulation to be less than 1.1% of cross feed from other charmless $B\overline{B}$ modes. The charmless events (henceforth refered to as $B\overline{B}$) have ultimate final states different from the signal, but similar kinematics, and exhibit broad peaks in the signal regions of some observables. We account for these with a separate component in the probability density function (PDF). For each component j (signal, $q\overline{q}$ combinatorial background, or $B\overline{B}$ background) and tagging category c, we define a total probability density function for event i as

$$\mathcal{P}^i_{j,c} \equiv \mathcal{P}_j({m_{\rm ES}}^i) \cdot \mathcal{P}_j(\Delta E^i) \cdot \mathcal{P}_j(\mathcal{F}^i) \cdot \mathcal{P}_j(\Delta t^i, \sigma^i_{\Delta t}; c)\,, \tag{2}$$

except for $B^0 \to \eta' K^0_L$ for which $\mathcal{P}_j({m_{\rm ES}}^i)$ is omitted. The factored form of the PDF is a good approximation, particularly for the combinatorial $q\overline{q}$ component, since correlations among observables measured in the data (in which $q\overline{q}$ dominates) are small. Distortions of the fit results caused by this approximation are measured in simulation and included in the bias corrections and systematic errors discussed below.

With Y_j defined to be the yield of events of component j, and $f_{j,c}$ the fraction of events of component j for each category c, we write the extended likelihood function for all events belonging to category c as

$$\mathcal{L}_c = \exp\Big(-\sum_j Y_j f_{j,c}\Big) \prod_i^{N_c} (Y_{\rm sig} f_{{\rm sig},c} \mathcal{P}^i_{{\rm sig},c} + Y_{q\bar{q}} f_{q\bar{q},c} \mathcal{P}^i_{q\bar{q}} + Y_{B\bar{B}} f_{B\bar{B},c} \mathcal{P}^i_{B\bar{B}}), \tag{3}$$

where N_c is the number of events of category c in the sample. We found that the $B\overline{B}$ background component is needed only for the channels with $\eta'_{\rho\gamma}$. We fix both $f_{{\rm sig},c}$ and $f_{B\bar{B},c}$ to $f_{B_{\rm flav},c}$, the values measured with the large $B_{\rm flav}$ sample [21]. The total likelihood function $\mathcal{L}_d$ for decay mode d is given as the product over the six tagging categories. Finally, when combining decay modes we form the grand likelihood $\mathcal{L} = \prod \mathcal{L}_d$.

The PDF $\mathcal{P}_{\rm sig}(\Delta t, \sigma_{\Delta t}, c)$ is given by $F(\Delta t)$ (Eq. 1) with tag category (c) dependent mistag parameters convolved with the signal resolution function (a sum of three Gaussians) determined from the $B_{\rm flav}$ sample. We determine the remaining PDFs for the signal and $B\overline{B}$ background components from fits to MC data, for which the resolutions in ΔE and $m_{\rm ES}$ are calibrated with large control samples of B decays to charmed final states of similar topology (e.g. $B \to D(K\pi\pi)\pi$). For the combinatorial background the PDFs are determined in the fits to the data. However we first deduce the functional form from a fit of each component alone to a sideband in $(m_{\rm ES}, \Delta E)$, so that we can validate the fit before applying it to data containing the signal.

These PDF forms are: the sum of two Gaussians for $\mathcal{P}_{\rm sig}(m_{\rm ES})$ and $\mathcal{P}_{\rm sig}(\Delta E)$; the sum of three Gaussians for $\mathcal{P}_{q\bar{q}}(\Delta t; c)$; a conjunction of two Gaussian segments below and above the peak with different widths for $\mathcal{P}_j(\mathcal{F})$ (a small "tail" Gaussian is added for $\mathcal{P}_{q\bar{q}}(\mathcal{F})$); a linear dependence for $\mathcal{P}_{q\bar{q}}(\Delta E)$; and for $\mathcal{P}_{q\bar{q}}(m_{\rm ES})$ the function $x\sqrt{1-x^2}\exp\left[-\xi(1-x^2)\right]$, with $x \equiv 2m_{\rm ES}/\sqrt{s}$. These are discussed in more detail in [10].

We allow the parameters most important for the determination of the combinatorial background PDFs to vary in the fit. Thus for the six channels listed in Table 2 we perform a single fit with

109 free parameters: $-\eta S$, C, signal yields (6), $\eta'_{\rho\gamma}K^0$ $B\overline{B}$ background yields (2), continuum background yields (6) and fractions (30), background Δt, $m_{\rm ES}$, ΔE, $\mathcal{F}$ PDF parameters (63). The parameters τ and Δm_d are fixed to world-average values [20]. The symbol S refers to $S_{\eta' K^0_S}$, and inclusion of the CP eigenvalue η of the final state accounts for the expected difference in sign with respect to $\eta' K^0_L$.

We test and calibrate the fitting procedure by applying it to ensembles of simulated $q\overline{q}$ experiments drawn from the PDF into which we have embedded the expected number of signal and $B\overline{B}$ background events randomly extracted from the fully simulated MC samples. We find negligible bias for C. For S we find and apply multiplicative correction factors for bias from dilution due to $B\overline{B}$ background, equal to 1.02 in the final states $\eta'_{\rho\gamma}K^0_{\pi^+\pi^-}$ and $\eta'_{\eta_{\gamma\gamma}\pi\pi}K^0_L$, and 1.05 in $\eta'_{\rho\gamma}K^0_{\pi^0\pi^0}$.

3.5 Fit Results

Table 2: Results with statistical errors for the $B^0 \to \eta' K^0$ time-dependent fits.

Mode	Events to fit	Signal yield	$-\eta S$	C
$\eta'_{\eta(\gamma\gamma)\pi\pi}K^0_{\pi^+\pi^-}$	612	206 ± 16	0.60 ± 0.24	-0.26 ± 0.14
$\eta'_{\rho\gamma}K^0_{\pi^+\pi^-}$	10905	503 ± 28	0.50 ± 0.15	-0.26 ± 0.11
$\eta'_{\eta(3\pi)\pi\pi}K^0_{\pi^+\pi^-}$	164	63 ± 8	0.85 ± 0.38	0.24 ± 0.26
$\eta'_{\eta(\gamma\gamma)\pi\pi}K^0_{\pi^0\pi^0}$	446	50 ± 9	0.77 ± 0.44	-0.25 ± 0.36
$\eta'_{\rho\gamma}K^0_{\pi^0\pi^0}$	12559	114 ± 23	0.42 ± 0.47	0.30 ± 0.30
$\eta' K^0_S$			0.57 ± 0.11	-0.18 ± 0.08
$\eta' K^0_L$	3389	168 ± 21	0.39 ± 0.30	0.20 ± 0.23
$\eta' K^0$			0.55 ± 0.11	-0.15 ± 0.07

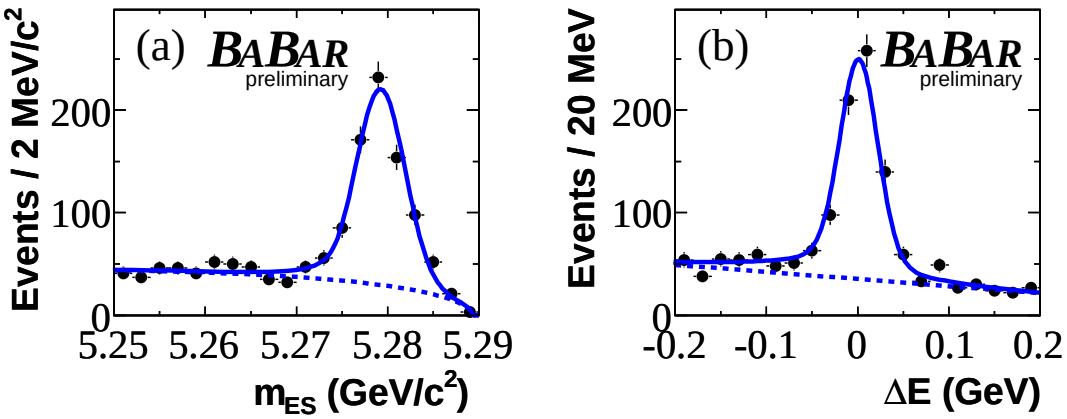

Figure 1: Distributions projected onto (a) $m_{\rm ES}$ and (b) ΔE for $B^0 \to \eta' K^0_S$ candidates.

Results from the fit for the signal yields and the CP parameters S and C are presented in Table 2. In Fig. 1 we show for $B^0 \to \eta' K^0_S$ the projections onto $m_{\rm ES}$ and ΔE for a subset of the data for which the signal likelihood (computed without the variable plotted) exceeds a mode-dependent threshold that optimizes the sensitivity; the corresponding distribution in ΔE for $B^0 \to \eta' K^0_L$ is

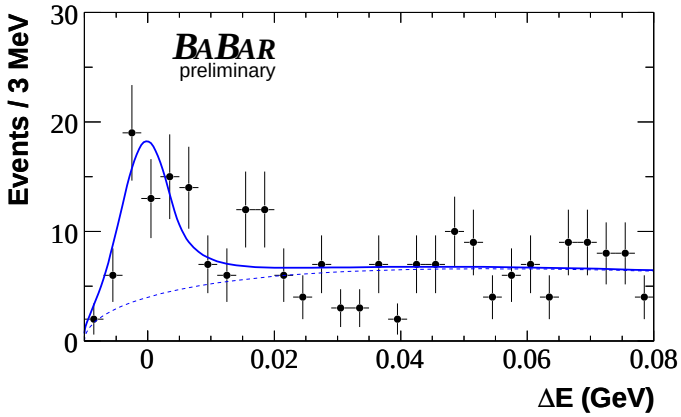

Figure 2: Distribution projected onto ΔE for $B^0 \to \eta' K^0_L$ candidates. Points with error bars represent the data, the solid line the fit function, and the dashed line its background component.

given in Fig. 2. Fig. 3 gives the Δt projections and asymmetry of the combined modes for events selected as for Figs. 1 and 2. We measure a correlation of 3.0% between S and C in the fit.

We perform numerous crosschecks of our fitter: time-dependent fits for B^+ decays to the charged final states $\eta'_{\eta(\gamma\gamma)\pi\pi}K^+$, $\eta'_{\rho\gamma}K^+$, and $\eta'_{\eta(3\pi)\pi\pi}K^+$; fits removing one fit variable at a time; fits without $B\overline{B}$ PDFs; fits with multiple $B\overline{B}$ components; fits allowing for non-zero CP information in $B\overline{B}$ events; fits with $C = 0$ and others. In all cases, we find results consistent with expectation. The value $S_{\eta' K^0_S} = 0.57 \pm 0.11$ is larger than our previous measurement $S_{\eta' K^0_S} = 0.30 \pm 0.14$ [13] as a result of the larger data sample and events added or removed as a result of changes in the reconstruction and selection. For events common to the two datasets we find close agreement of the values of S and C.

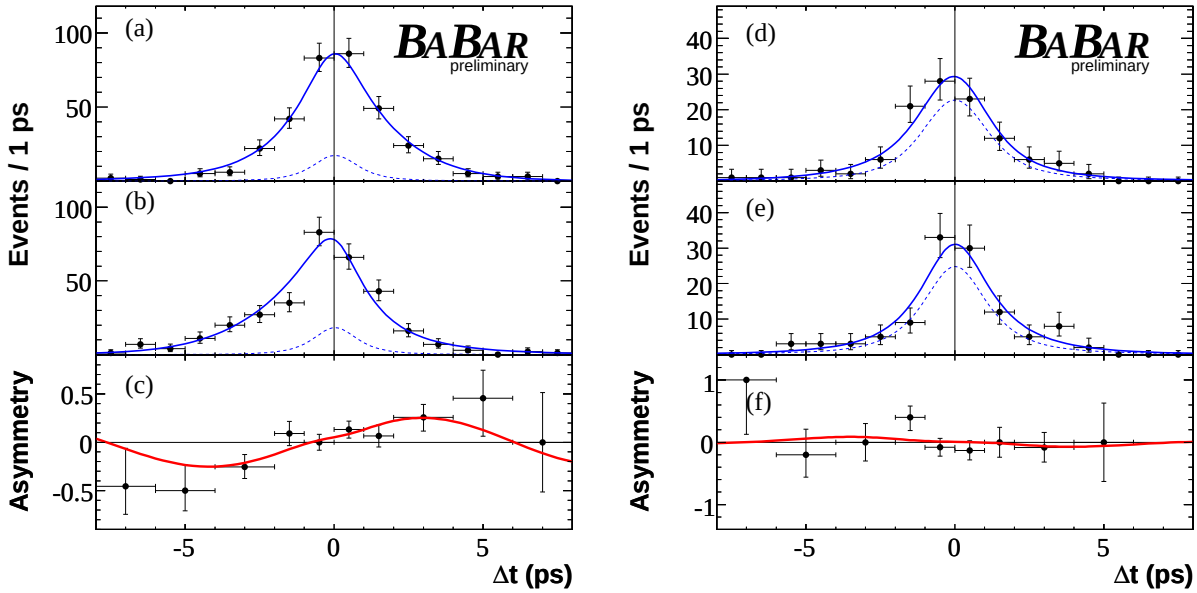

Figure 3: Projections onto Δt for (a-c) $B^0 \to \eta' K^0_S$ and (d-f) $B^0 \to \eta' K^0_L$ of the data (points with error bars), fit function (solid line), and background function (dashed line), for (a, d) B^0 and (b, e) $\overline{B}^0$ tagged events, and (c, f) the asymmetry between B^0 and $\overline{B}^0$ tags.

3.6 Systematic studies

We find systematic uncertainties from several sources (in decreasing order of magnitude): variation of the signal PDF shape parameters within their errors, modeling of the signal Δt distribution, use of Δt signal parameters from the $B_{\rm flav}$ sample, interference between the CKM-suppressed $\bar{b} \to \bar{u}c\bar{d}$ amplitude and the favored $b \to c\bar{u}d$ amplitude for some tag-side B decays [22], $B\overline{B}$ background, SVT alignment, and position and size of the beam spot. The $B_{\rm flav}$ sample is used to determine the errors associated with the signal Δt resolutions, tagging efficiencies, and mistag rates. We take the uncertainties in τ_B and Δm_d from the published measurements [20]. Summing all systematic errors in quadrature, we obtain 0.02 for S and 0.03 for C.

4 RESULTS AND DISCUSSION

In conclusion, we have used samples of about 940 $B^0 \to \eta' K^0_S$ and 170 $B^0 \to \eta' K^0_L$ events to measure the time-dependent *CP* violation parameters in $B^0 \to \eta' K^0$ $S = 0.55 \pm 0.11 \pm 0.02$ and $C = -0.15 \pm 0.07 \pm 0.03$. Our result for S is consistent with the world average of those measured in $B^0 \to J/\psi K^0_S$ [18, 15], and inconsistent with zero (*CP* conservation) by 4.9 standard deviations. Our result for the direct-*CP* parameter C is 1.8 standard deviations from zero. The results are preliminary.

5 ACKNOWLEDGMENTS

We are grateful for the extraordinary contributions of our PEP-II colleagues in achieving the excellent luminosity and machine conditions that have made this work possible. The success of this project also relies critically on the expertise and dedication of the computing organizations that support *BABAR*. The collaborating institutions wish to thank SLAC for its support and the kind hospitality extended to them. This work is supported by the US Department of Energy and National Science Foundation, the Natural Sciences and Engineering Research Council (Canada), Institute of High Energy Physics (China), the Commissariat à l'Energie Atomique and Institut National de Physique Nucléaire et de Physique des Particules (France), the Bundesministerium für Bildung und Forschung and Deutsche Forschungsgemeinschaft (Germany), the Istituto Nazionale di Fisica Nucleare (Italy), the Foundation for Fundamental Research on Matter (The Netherlands), the Research Council of Norway, the Ministry of Science and Technology of the Russian Federation, Ministerio de Educación y Ciencia (Spain), and the Particle Physics and Astronomy Research Council (United Kingdom). Individuals have received support from the Marie-Curie IEF program (European Union) and the A. P. Sloan Foundation.

References

[1] *BABAR* Collaboration, B. Aubert *et al.*, Phys. Rev. Lett. **89**, 201802 (2002); Belle Collaboration, K. Abe *et al.*, Phys. Rev. D **66**, 071102(R) (2002).

[2] N. Cabibbo, Phys. Rev. Lett. **10**, 531 (1963); M. Kobayashi and T. Maskawa, Prog. Theor. Phys. **49**, 652 (1973).

[3] Y. Grossman and M. P. Worah, Phys. Lett. B **395**,241 (1997); D. Atwood and A. Soni, Phys. Lett. B **405**, 150 (1997).

[4] Y. Grossman *et al.*, Phys. Rev. D **68**, 015004 (2003).

[5] C.-W. Chiang, M. Gronau and J. L. Rosner, Phys. Rev. D **68**, 074012 (2003).

[6] M. Gronau, J. L. Rosner and J. Zupan, Phys. Lett. B **596**, 107 (2004).

[7] M. Beneke and M. Neubert, Nucl. Phys. B **675**, 333 (2003).

[8] D. London and A. Soni, Phys. Lett. B **407**, 61 (1997).

[9] *BABAR* Collaboration, B. Aubert *et al.*, Phys. Rev. Lett. **93**, 181806 (2004); Belle Collaboration, P. Chang *et al.*, Phys. Rev. D **71**, 091106 (2005).

[10] *BABAR* Collaboration, B. Aubert *et al.*, Phys. Rev. D **70**, 032006 (2003).

[11] *BABAR* Collaboration, B. Aubert *et al.*, Phys. Rev. D **73**, 071102 (2006).

[12] Our implementation of the ΔS calculation follows the method described in *BABAR* Collaboration, B. Aubert *et al.*, hep-ex/0606050 (2006).

[13] *BABAR* Collaboration, B. Aubert *et al.*, Phys. Rev. Lett. **94**, 191802 (2005); BABAR-CONF-05/14 [hep-ex/0507087].

[14] Belle Collaboration, K. Abe *et al.*, Phys. Rev. D **72**, 012004 (2005).

[15] Belle Collaboration, K. Abe, *et al.*, BELLE-CONF-0569 [hep-ex/0507037] (2005).

[16] *BABAR* Collaboration, B. Aubert *et al.*, Nucl. Instr. Methods Phys. Res., Sect. A **479**, 1 (2002).

[17] PEP-II Conceptual Design Report, SLAC-R-418 (1993).

[18] *BABAR* Collaboration, B. Aubert *et al.*, Phys. Rev. Lett. **94** 161803 (2005).

[19] The *BABAR* detector Monte Carlo simulation is based on GEANT4: S. Agostinelli *et al.*, Nucl. Instr. Methods Phys. Res., Sect. A **506**, 250 (2003).

[20] Particle Data Group, Y.-M. Yao et al., J. Phys. **G33**, 1 (2006).

[21] *BABAR* Collaboration, B. Aubert *et al.*,Phys. Rev. D **66**, 032003 (2002).

[22] O. Long *et al.*, Phys. Rev. D **68**, 034010 (2003).